Applied Radiation and Isotopes 69 (2011) 1002–1006

Contents lists available at ScienceDirect

Applied Radiation and Isotopes

journal homepage: www.elsevier.com/locate/apradiso

Synthesis of $CaSO_4$: Mn nanosheets with high thermoluminescence sensitivity

Mostafa Zahedifar [a,b,*], Mohsen Mehrabi [b], Somayeh Harooni [a]

[a] TL Laboratory Physics Department, University of Kashan, Kashan, Iran
[b] Institute of Nanoscience and Nanotechnology, University of Kashan, Kashan, Iran

ARTICLE INFO

Article history:
Received 16 June 2010
Received in revised form
19 January 2011
Accepted 25 January 2011
Available online 7 April 2011

Keywords:
Nanosheets
$CaSO_4$:Mn
Thermoluminescence
High sensitivity

ABSTRACT

Nanosheet $CaSO_4$:Mn having an average thickness of 35 nm was synthesized by the hydrothermal method and its thermoluminescence (TL) and photoluminescence (PL) characteristics were studied. Three overlapping TL glow peaks were identified in the complex glow curve using the T_{stop} technique. Activation energies of 3.76, 2.22 and 2.47 eV and kinetic orders of 1.01, 1.20 and 1.99 were found for three component glow peaks at 485, 504 and 526 K, respectively, using a computerized glow curve deconvolution procedure. An emission spectra band at 497 nm was observed for the synthesized nanosheet. The thermoluminescence sensitivity of the prepared nanocrystallite was found to be around eight times higher than that of LiF:Mg,Cu,P (GR-200) hot-pressed chips. Dosimetric properties of this phosphor, including dose response, fading and reusability, are also presented.

1. Introduction

Thermoluminescence is a well known phenomenon used for the dosimetry of ionizing radiations. The energy absorbed by a TL material during irradiation is released as visible and UV light on subsequent heating of the sample. It has been found that the intensity and area of stable TL glow peaks are (within a definite range) proportional to the received dose and this is the basis of dosimetry of ionizing radiations by TL phosphors. The properties of common TL materials have been optimized for measurements of ionizing radiations and there are many commercially available dosimeters (TLDs) with different trade names (McKeever, 1985). Currently nanotechnology has attracted numerous researchers from different fields (Nalwa, 2000). It has been established that the optical properties of materials on nanoscale can be very different from those of their bulk equivalent (Salah et al., 2006a, 2006b). These studies state that the aforesaid materials have a potential application in dosimetry of ionizing radiations for high dose levels where the conventional microcrystalline phosphors are not applicable (Lochab et al., 2007a, 2007b; Sahare et al., 2007). Decreasing the size of particles causes increasing of both the number of surface states and proportion of recombination of charge carriers. Reports on TL properties of nanomaterials show that they include some outstanding characteristics such as high sensitivity and saturation at very high dose levels (Dela Rosa et al., 2007; Kumar et al., 2006; Pandey et al., 2003; Rodriguez et al., 2005). Singly doped $CaSO_4$ has been studied in detail in the past and two models have been presented for TL mechanism in $CaSO_4$ based TL phosphors (Bhatt et al., 2006; Ingle et al., 2008; Madhusoodanan et al., 1999; Menon et al., 2005; Rivera et al., 2010). The TL properties of $CaSO_4$:Dy nanoparticles have been studied recently (Salah et al., 2006a) but no report is available on the TL of nanostructured $CaSO_4$:Mn. This study is focused on preparation and investigation of TL properties of $CaSO_4$:Mn nanosheets.

2. Experiment

2.1. Method of preparation

The hydrothermal method was used for preparing $CaSO_4$:Mn nanosheets. The raw materials used for synthesis of $CaSO_4$:Mn nanosheets were $(C_2H_3COO)_2Ca$ (Merk) 99%, $(MnSO_4)\cdot 2H_2O$ 99.9% (Merk), $(NH_4)_2SO_4$ 99% (Merk), Brij 35 99.9% (Merk), C_2H_5OH 99.9% (Merk) and distilled deionized water (Merk). First a solution of calcium acetate was prepared in two stages as follows:

(a) 0.3954 g of $(C_2H_3COO)_2Ca$ was dissolved in 50 ml distilled deionized water and stirred for 15 min. (b) 4.5 g of Brij 35 surfactant was dissolved in a mixture of 40 ml deionized water and 10 ml ethanol and the resulting solution was mixed with calcium acetate solution prepared in stage (a) and was placed on a stirrer for 15 min. Then different amounts of manganese sulfate were added to the solution. Finally 0.025 mol of ammonium

* Corresponding author at: Physics department, University of Kashan, Kilometer 6, Ravand Boulevard, Kashan, Isfahan 8731751167, Iran. Tel.: +98 361 5514005; fax: +98 361 5552930.
E-mail address: zhdfr@kashanu.ac.ir (M. Zahedifar).

0969-8043/$ - see front matter © 2011 Elsevier Ltd. All rights reserved.
doi:10.1016/j.apradiso.2011.01.036

sulfate solution was prepared by dissolving 0.3035 g of $(NH_4)_2SO_4$ in 100 ml distilled deionized water and was added slowly to calcium acetate solution obtained in stage (b). The mixture was placed in an autoclave at 180 °C for 24 h. The solid part was collected by centrifuging the mixture and was thoroughly washed with ethanol. The collected nanostructures were then dried in an oven for 2 h followed by annealing at 300 °C for 1 min under nitrogen atmosphere. The final product was $CaSO_4$:Mn nanosheets. It is worth noting that formation of nanosheets is highly dependent on duration of storage of the final mixture in autoclave at 180 °C. Reduction of time from 24 to12 h results in the formation of nanoparticles (quantum dots), but thermoluminescence sensitivity of produced nanoparticles is found to be two times lower than that of nanosheets. Therefore we concentrated on studying the properties of nanosheets.

2.2. Sample analysis

The structural characterization of nanosheets was supported by X-ray diffraction (XRD) with a Rigaku D-maxcIII diffractometer using Cu K_α radiations. SEM images were obtained using a scanning electron microscope model Philips XL-30 ESEM equipped with an energy dispersive spectrometer (EDS). Doses of ionizing radiation were administrated to the samples in air under electronic equilibrium conditions with a ^{137}Cs gamma source that had been calibrated against a ^{60}Co photon source at the secondary standard dosimetry laboratory (SSDL) facilities, Karaj, Iran. The TL readouts were taken in a Harshaw model 4500 computer based TL reader using contact heating, where the temperature of the heater strip (planchet) was recorded as an indicator of temperature of the sample. Pre-irradiation annealing procedure was performed by heating the sample at 300 °C for 1 min under nitrogen atmosphere and rapid cooling to room temperature. All of the samples were kept in dark condition in the time interval between annealing and readout. For reducing the thermal lag across the powder sample, low heating rate of 1 °C/s was used for recording the glow curves with preheating at 50 °C to a maximum temperature of 320 °C in nitrogen atmosphere. Because of stability (negligible fading) of glow peaks of this phosphor, the total glow curve area was used in TL readout process. TL response to a specific absorbed dose was measured as an average over four readouts of samples of the same mass. The precession in the measurements of TL response was better than 3%. PL spectrum was recorded using a spectrometer model Perkin Elmer LS55 with a photomultiplier tube and a Xenon lamp at room temperature.

3. Results

3.1. SEM, EDS and XRD results

Fig. 1 shows the XRD pattern of the $CaSO_4$:Mn nanosheets. This spectrum reveals that the sample is $CaSO_4$ with orthorhombic structure and corresponds to JCPDS card no. 06-0226. Assuming that the nanosheets are stress free, the effective thickness of nanosheets was calculated by the Scherer formula from the broadening of the (0 2 0) peak in the XRD pattern (Cullity, 1956). The average thickness of the (0 2 0) plane was estimated to be approximately 35 nm, which agrees well with the SEM images. The SEM photograph of nanosheets and nanoparticles is shown in Fig. 2 and EDS spectrum of nanosheets is illustrated in Fig. 3.

3.2. PL spectra

Fig. 4 shows the PL emission spectrum of the nanosheets sample with a maximum at 497 nm while the PL pattern of bulk $CaSO_4$:Mn has a peak at $\approx$500 nm. The bulk phosphor exhibits distinct

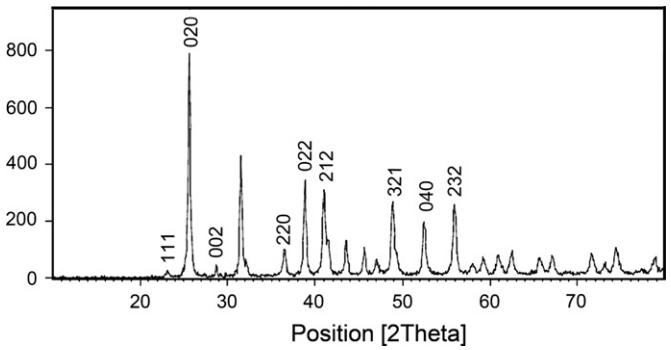

Fig. 1. XRD pattern of the synthesized nanosheets.

excitation bands at 110 and 150 nm. The 110 nm band is due to valence band–conduction band excitation in $CaSO_4$ as its band gap is around 11–12 eV (Lakshmanan, 2008). The weak blueshifting of emission wavelengths is due to the quantum size effect, i.e. a decrease in particle size results in reduction of the number of allowed transitions to some extent in the nanocrystallite.

3.3. Thermoluminescence glow curve

$CaSO_4$:Mn microcrystallite shows a single TL glow peak around 100 °C, which does not resemble the glow curves of rare earth (RE) doped $CaSO_4$ (main peak around 200 °C). The 200 °C TL peak in RE doped $CaSO_4$ is correlated with the holes trapped by sulphate radicals near Ca^{2+} ion vacancies created due to charge imbalance between RE^{3+} ions and Ca^{2+} ions. Since the incorporation of Mn^{2+} ions does not create cation vacancies, the high temperature TL peak is absent in bulk $CaSO_4$:Mn (Menon et al., 2005). Fig. 5 shows the TL glow curve of $CaSO_4$:Mn nanosheets exposed to γ-rays from ^{137}Cs source (open circles), which contains three overlapping peaks around 485, 504 and 526 K. Comparison of glow curves of nano- and microcrystallites shows that the number of glow peaks is increased in the nanocrystallite. Considering the SO_4^- and SO_3^- host ions as hole traps, this discrepancy can be related to surface active hole traps in nanocrystallite, i.e. by decreasing the size of the particles, the ratio of area to volume increases significantly, which results in considerable increase of surface hole traps having different trap characteristics. Also the sensitivity of glow peaks drastically increased in nanocrystalline phosphor compared with microcrystalline phosphor. But in some cases the TL sensitivity of the nanocrystalline phosphor is less than that of its corresponding microcrystalline phosphor (Salah et al., 2006a, 2006b). The T_{stop} method was employed for identifying the number of glow peaks contained in the complex glow curve of the synthesized nanosheets. Using this method, the TL glow curves were recorded after post-irradiation anneal up to T_{stop} in the range of 460–570 K. In Fig. 6 the variation of T_m (the temperature of peak maximum) vs T_{stop} is presented. As is evident, by increasing T_{stop} the main glow peak moves towards higher temperatures, but this variation is not monotonic and several jumps are observed in T_m. The regions in which T_m does not change abruptly belong to a single glow peak. Three of such zones can be distinguished in this figure. A computerized glow curve deconvolution (CGCD) technique was used for obtaining the trapping parameters of the three overlapping glow peaks. The computer program has been produced in our laboratory using the Levenberg–Marquart algorithm based on non-linear least square method. Thermoluminescence general order kinetics model was employed in our program for curve fitting. In the CGCD procedure, we exploited a glow curve deconvolution function in terms of I_m, T_m, b, E instead of s, n_o, b, E (n_o, cm^{-3} is the initial population of trapping states) since I_m and T_m can be easily estimated

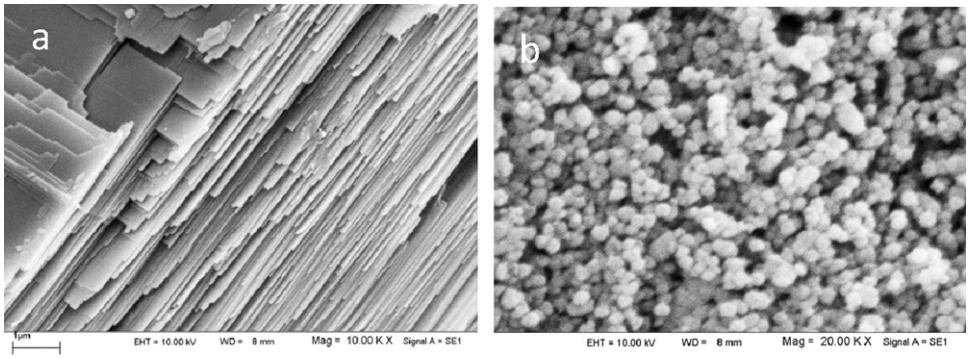

Fig. 2. SEM images of produced nanosheets (a) and nanoparticles (b).

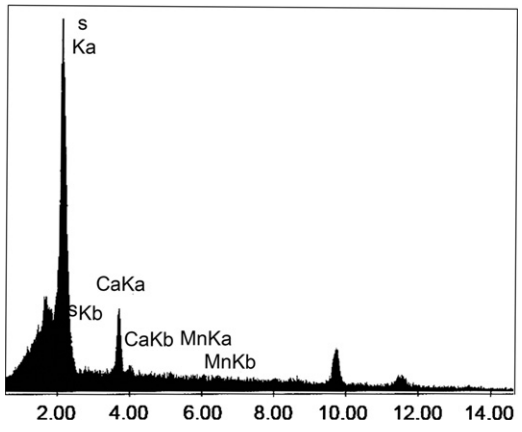

Fig. 3. EDS spectra of synthesized nnanosheets.

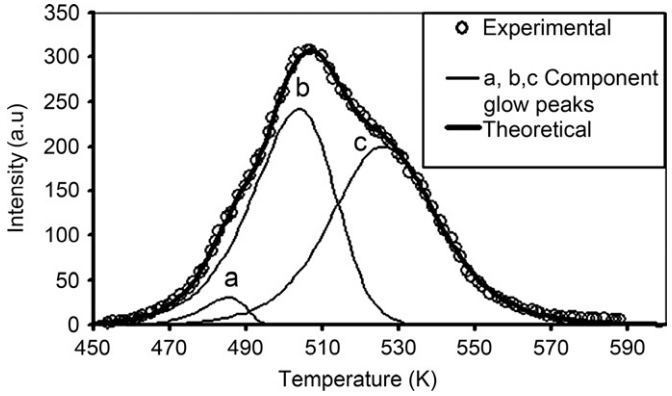

Fig. 5. Thermoluminescence glow curve of nanosheets (open circles) and component glow peaks (solid lines) obtained using computerized glow curve deconvolution.

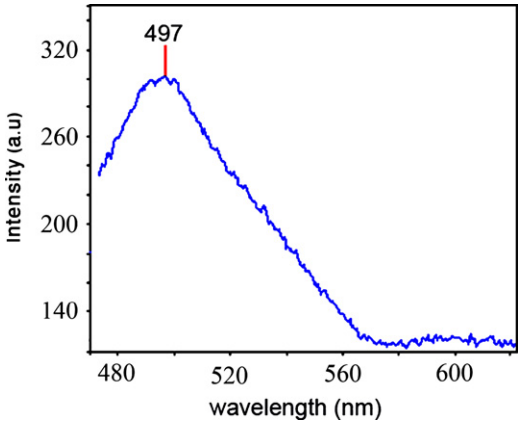

Fig. 4. Photoluminescence spectra of prepared nanosheets.

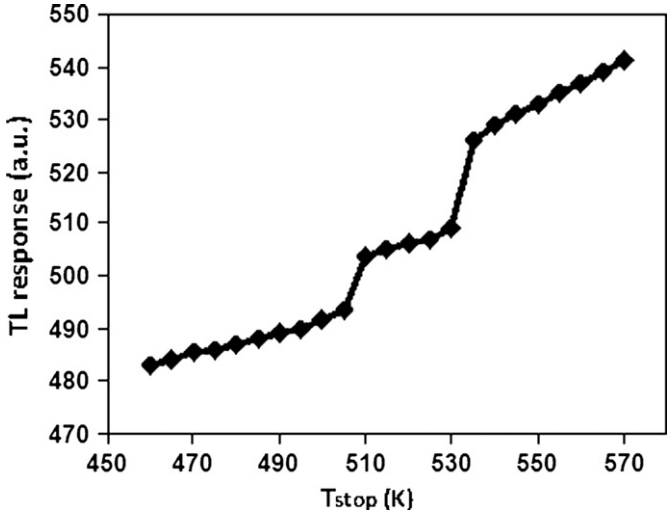

Fig. 6. Variation of temperature of peak maximum, T_m vs. T_{stop} for the synthesized nanosheets.

from the shape of the glow curve as initial values in glow curve deconvolution process. The TL intensity in terms of I_m and T_m (the intensity and the temperature of peak maximum) is (Kitis et al., 1998)

$$I(T) = I_m b^{b/b-1} \exp\left(\frac{E}{kT}\frac{T-T_m}{T_m}\right) \times \left[(b-1)(1-\Delta)\frac{T^2}{T_m^2}\exp\left(\frac{E}{kT}\frac{T-T_m}{T_m}\right)+Z_m\right]^{-b/b-1} \quad (1)$$

in which b is the order of kinetics, E the activation energy, k the Boltzmann constant, T the temperature, $\Delta = 2kT/E$, $\Delta_m = 2kT_m/E$ and $Z_m = 1+(b-1)\Delta_m$. For testing the goodness of fit, the figure of merit (FOM) has been used (Balian and Eddy, 1977):

$$FOM = \sum_{j_f}^{j_l} \frac{100[y_i - y(x_i)]}{A} \quad (2)$$

in which j_f and j_l are the numbers of the first and last temperature interval ΔT used for curve fitting, respectively, Y_i is the intensity in the

ith interval obtained from experiment, $Y(x_i)$ the intensity expected from Eq. (1) and A the total area of fitted glow peak between j_f and j_i.

A relatively low FOM value of 1.23% is indication of good fittness of experimental and the theoretical peaks based on general order of kinetics. The component glow peaks are also shown in Fig. 5. The activation energy, kinetic order and maximum temperature of the three mentioned peaks are presented in Table 1. As is seen the activation energy of peak (a) is above 3 eV, which is extremely high and outside of the physical accepted limits. Kitis and Otto (2000) have reported the activation energy even greater than 3 eV for peak 5a of LiF:Mg,Ti (TLD-100) which appears as a shoulder of peak 5. They also proposed a model responsible for the artificial narrowing of experimentally observed glow peak 5a. The main characteristic of this peak is that its FWHM (full width at half maximum) is less than 20 °C. Considering the inverse relationship between activation energy and FWHM, the estimated activation energy will be greater than the expected value. Chen and Hag-Yahya (1996) in their proposed TL model based on one trapping center and three recombination centers suggested that the very high activation energy associated with peak 5 could be due to narrowing of the peak shape caused by competition in the excitation stage and heating stage. The high activation energy obtained in this study is justified by the low value of FWHM (about 15 °C) achieved for the weak glow peak (a) of the synthesized nanosheets, as shown in Fig. 5. The effect of Mn concentration on TL sensitivity of nanocrystalline is illustrated in Fig. 7. As mentioned in experimental section, the TL response of produced nanosheets was analyzed at different added values of Mn to the solution. The results depicted in Fig. 7 reveal the maximum sensitivity yields for 0.4 mol% of Mn impurity. Fig. 8 shows the dose response of the synthesized nanosheets. As is seen, the response is linear up to the absorbed dose of about 7 Gy before saturation. For testing the fading of glow curve, nanosheet samples were annealed (300 °C for 1 min) and irradiated to a dose of 0.5 Gy of ^{137}Cs. The stability of the stored TL signal was studied using 28 samples in 7 groups. The groups were irradiated and stored in dark at room temperature (≈ 25 °C) prior to reading out. Fig. 9 shows that the reduction of response is negligible up to 1 month of storing the phosphor at room temperature. Also the thermoluminescence sensitivity of $CaSO_4$:Mn nanosheets was compared with the high sensitive LiF:Mg,Cu,P hot pressed chips (GR-200) for identical irradiation conditions. The TL sensitivity is expressed as glow curve area per unit mass of the phosphor and unit of absorbed dose of gamma rays. As is shown in Fig. 10, the TL sensitivity of the synthesized $CaSO_4$:Mn nanosheets is around eight times higher than that of GR-200 phosphor. The sensitivity of LiF:Mg,Cu,P is approximately 25 times higher than that of LiF:Mg,Ti (TLD-100) (Moscovitch and Horowitz, 2007). Therefore, the TL sensitivity of the produced nanosheets is about 200 times higher than that of LiF:Mg,Ti. The TL phosphor Mg_2SiO_4:Tb with the sensitivity of 110 times higher than that of LiF:Mg,Ti (TLD-100) has been reported as one of the most sensitive thermoluminescence phosphors prepared so far

Table 1
Activation energy (E), peak maximum temperature (T_m) and order of kinetics (b) of 3 isolated glow peaks contained in complex glow curve of nanosheets.

Peak	E (eV)	T_m (K)	I_m	b
a	3.76	485	30.9231	1.01
b	2.22	504	240.7385	1.20
c	2.47	526	199.5768	1.99

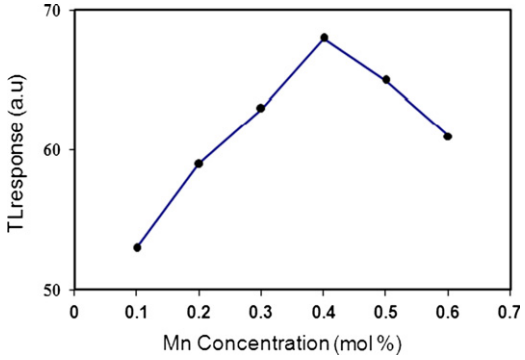

Fig. 7. Effect of concentration of Mn dopant on thermoluminescence response of nanosheets.

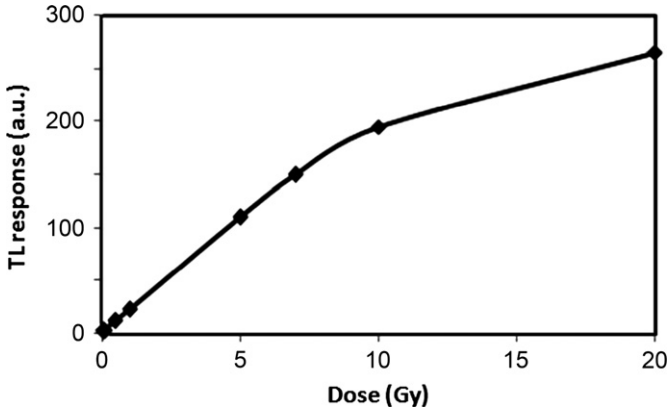

Fig. 8. Dose response of the $CaSO_4$:Mn nanosheets.

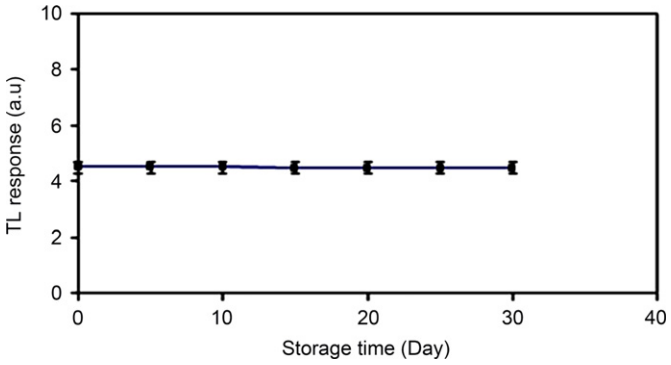

Fig. 9. TL response of the $CaSO_4$:Mn nanosheets against the storage time at room temperature.

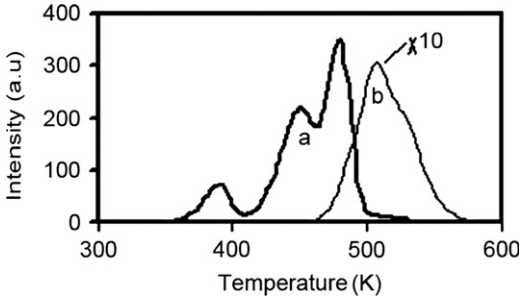

Fig. 10. Comparison of the TL glow curves of LiF:Mg,Cu,P (GR-200) commercial phosphor (a) and the $CaSO_4$:Mn nanosheets (b) for the absorbed dose of 5 Gy from the ^{137}Cs gamma source. The heating rate used for recording the TL glow curves is 1 °C/s. The symbol × 10 implies that the intensity is to be multiplied by a factor of 10.

(Prokic and Yukihara, 2008). Results presented here demonstrate that the sensitivity of prepared nanosheets is even about 2 times more than that of high sensitive Mg_2SiO_4:Tb TL phosphor. Also the reusability of the synthesized nanosheets was tested by 10 successive cycles of annealing, irradiation and readout of the same sample. The reduction in sensitivity was negligible after 10 cycles of sample readout. TL response of the synthesized nanosheets to photon energies from the ^{137}Cs and ^{60}Co gamma sources was exactly the same. The TL response to lower energy photon fields is under investigation.

Conclusions

The TL glow curve of bulk $CaSO_4$:Mn has one peak around 373 K, while the number of component peaks in our synthesized nanosheets was increased. A TL glow peak is representative of a special trapping center in band gap. In $CaSO_4$:Mn TL phosphor, decreasing the particle size results in an increase in the band gap, which also causes the reformation of associated states of impurities. Also, creation of surface active traps in going from micro- to nanoscale (which is a result of increasing of surface to volume fraction) seems to be responsible for increasing the number of glow peaks contained in TL glow curve of nanostructured phosphor. Manganese doped bulk $CaSO_4$ has been found to have a very high sensitivity, but it cannot be used in radiation dosimetry due to considerable fading (Menon et al. 2005). Our synthesized nanosheets, besides having negligible fading due to stable higher temperature peaks, has much TL sensitivity compared to its bulk equivalent. The strong enhancement in TL sensitivity can be attributed to considerable overlapping of the wave functions of electrons and holes on decreasing the size of the particles, which results in an increase in their recombination probability. In summary, because of easier preparation, very good sensitivity (200 times higher than that of LiF:Mg,Ti), very low fading and excellent reusability, the synthesized $CaSO_4$:Mn nanosheets are recommended as a good candidate for application in environmental radiation dosimetry.

References

Balian, H.G., Eddy., N.W., 1977. Figure-of-merit (FOM), an improved criterion over the normalized chi-squared test for assessing goodness of-fit of gamma-ray spectra peaks. Nucl. Instrum. Methods 145, 389–393.

Bhatt, B.C., Dhabekar., Bhushan, Kumar., Rajesh, Gundu Rao., T.K., Lakshmanan., A.R., 2006. Defect centers and thermoluminescence in $CaSO_4$:Dy,Ag phosphor. Radiat. Prot. Dosimetry 119, 53–56.

Chen, R., Hag-Yahya, A., 1996. Interpretation of very high activation energies and frequency factors in TL as being due to competition between centers. Radiat. Prot. Dosimetry 65, 17–20.

Cullity, B.D., 1956. Elements of X-ray Diffraction 2nd ed. Addison–Wesley Publishing Company, p. 99.

Dela Rosa, E., Rodríguez, R.A., Meléndrez, R., Salas, P., Diaz-Torres, L.A., Barboza-Flores, M. 2007. Thermoluminescence properties of undoped and Tb^{3+} and Ce^{3+} doped YAG nanophosphor under UV-, X- and β-ray irradiation. Nucl. Instrum. Methods B. 255, 357–364.

Ingle, N.B., Omanwar, S.K., Muthal, P.L., Dhopte, S.M., Kondawar, V.K., Gunduraod, T.K., Moharil, S.V., 2008. Synthesis of $CaSO_4$:Dy, $CaSO_4$: Eu^{3+} and $CaSO_4$: Eu^{2+} phosphors. Radiat. Meas. 43, 1191–1197.

Kitis, G., Gomez Ros, J.M., Tuyn, J.W.N., 1998. Thermoluminescence glow-curve deconvolution functions for first, second and general order of kinetics. J. Phys. D Appl. Phys. 31, 2636.

Kitis, G., Otto, T., 2000. Peculiarities of the glow-peak 5a of LiF:Mg,Ti. Nucl. Instrum. Methods B 160, 262–273.

Kumar, V., Kumar, R., Lochab, S.P., Singh, N., 2006. Thermoluminescence and dosimetric properties of bismuth doped CaS nanocrystalline phosphor. Radiat. Eff. Defects Solids 161, 479–485.

Lakshmanan, A., 2008. Luminescence and Display Phosphors, Phenomena and Applications. Nova Science Publishers, Inc..

Lochab, S.P., Pandey, A., Sahare, P.D., Chauhan, R.S., Salah, N., Ranjan, R., 2007(. Nanocrystalline MgB_4O_7:Dy for high dose measurement of gamma radiation. Phys. Status Solidi 204, 2416–2425.

Lochab, S.P., Sahare, P.D., Chauhan, R.S., Salah., N., Pandey, A., 2007b. Thermoluminescence and photoluminescence study of nanocrystalline $Ba_{0.97}Ca_{0.03}SO_4$. Eu. J. Phys. D Appl. Phys. 40, 1343–1350.

Madhusoodanan, U., Jose, M.T., Tomita, A., Hoffmann, W., Lakshmanan, A.R., 1999. A new thermostimulated luminescence phosphor based on $CaSO_4$: Ag,Tm for applications in radiation dosimetry. J. Lumin. 82, 221–232.

McKeever, S.W.S., 1985. Thermoluminescence of Solids. Cambridge University Press, Cambridge.

Menon, S.N., Sanaye, S.S., Dhabekar, B.S., Kumar, Rajesh, Bhatt., B.C., 2005. Role of Mn as a co-dopant in $CaSO_4$:Mn,Pr TL phosphor. Radiat. Meas. 39, 111–114.

Moscovitch, M., Horowitz, Y.S., 2007. Thermoluminescent materials for medical applications: LiF:Mg,Ti and LiF:Mg,Cu,P. Radiat. Meas. 41, S71–S77.

Nalwa, H.S., 2000. Handbook of Nanostructured Materials and Nanotechnology, vols. 1–5. Academic, CA, San Diego.

Pandey, A., Sahare, P.D., Bakare, J.S., Lochab, S.P., Singh, F., Kanjilal, D., 2003. Thermoluminescence and photoluminescence characteristics of nanocrystalline $LiNaSO_4$:Eu phosphor. J. Phys. D Appl. Phys. 36, 2400–2406.

Prokic, M., Yukihara, E.G., 2008. Dosimetric characteristics of high sensitive Mg_2SiO_4:Tb solid TL detector. Radiat. Meas. 43, 463–466.

Rivera, T., Roman, J., Azorin, J., Guzman, J., Serrano, A.k., Garcia, M., Alarcon, G., 2010. Preparation of $CaSO_4$:Dy by precipitation method to gamma radiation dosimetry. Appl. Radiat. Isot. 68, 623–625.

Rodriguez, R.A., De la Rosa, E., Melendrez, R., Salas, P., Castaneda, J., Felix, M.V., Barboza-Flores, M., 2005. Thermoluminescence characterization of nanocrystalline and single $Y_3Al_5O_{12}$ crystal exposed to β-irradiation for dosimetric applications. Opt. Mater. 27, 1240–1244.

Sahare, P.D., Ranjan, R., Salah, N., Lochab, S.P., 2007. $K_3Na(SO_4)_2$:Eu nanoparticles for high dose of ionizing radiation. J. Phys. D Appl. Phys. 40, 759–764.

Salah, N., Sahare, P.D., Lochab, S.P., Kumar, P., 2006a. TL and PL studies on $CaSO_4$: Dy nanoparticles. Radiat. Meas. 41, 40–47.

Salah, N., Sahare, P.D., Rupasov, A.A., 2006b. Thermoluminescence of nanocrystalline LiF:Mg, Cu, P. J. Lumin. 124, 357–364.